

Optimum Co-Design of Spectrum Sharing Between MIMO Radar and MIMO Communication Systems: An Interference Alignment Approach

Mohamed Rihan¹, Member, IEEE, and Lei Huang², Senior Member, IEEE

Abstract—A major challenge in designing a spectral co-existence between radar and communication systems is how to simultaneously provide efficient utilization of the shared spectrum while maintaining a reliable performance for both systems. Due to its flexibility in using linear independent waveforms and superiority in terms of target detection and estimation, the colocated multiple-input-multiple-output (MIMO) radars provide a paramount capability in realizing spectrum sharing with communication systems. In this paper, we consider the use of joint transmit and receive beamformers for both the MIMO radar and MIMO communication systems. Specifically, we design a two-tier alternating optimization spectrum sharing framework that is based on interference alignment (IA) approach. The effectiveness of spectrum sharing between radar and communication systems is guaranteed by mitigating the mutual interference signals in the shared spectral band. Subsequently, motivated by the excellent performance provided by IA in different wireless network scenarios, we propose a spectrum sharing framework that consists of a main iterative algorithm with two subalgorithms included within its operation. The first subalgorithm is used to maximize the signal-to-interference-plus-noise ratio of the radar system, whereas the second one is utilized to maximize the average sum-rate of the communication system. The main iterative algorithm is proposed to jointly optimize the transmit and receive beamforming filters of both systems by performing alternating optimization between the two subalgorithms. The convergences of the proposed algorithm and its subalgorithms are numerically verified. Simulation results are provided to confirm the superiority of the proposed framework for both systems.

Index Terms—MIMO-radar, spectrum sharing, interference alignment, MIMO communications, co-existence, alternating optimization.

I. INTRODUCTION

THE ongoing tremendous growth of mobile data traffic has attracted the attention of mobile network operators

(MNOs) recently and poses a big challenge on the way of future wireless networks [1]. MNOs are helping to fix this challenging issue partially through their increased investments in their infrastructure, e.g., ultra-dense deployment of small cells, and looking for more spectrum-efficient technologies, e.g., long term evolution-advanced (LTE-advanced) [2], massive multiple-input multiple-output (MIMO) [3], and non-orthogonal multiple access (NOMA) [4]. On the other hand, the standardization bodies worldwide focus their efforts toward devising various schemes of spectrum sharing and management. For instance, the federal communications commission (FCC) focuses on developing solutions that are able to share the spectrum between different federal spectrum users, such as defense and civilian radars, public sector and mobile operators [5]. Specifically, the FCC as well as national telecommunication and information administration (NTIA) have proposed the sharing of 150 MHz spectrum in 3.5 GHz band, previously assigned to radar applications, with the communication applications [6]. Unfortunately, when both the radar and communication systems share the same spectrum band, they exert mutual electromagnetic interference to one another, which may greatly degrade the quality of services (QoS) of both systems.

During the last decade, many spectrum sharing schemes have been suggested to enable the radar to get along with communication systems within the same spectral band. One of the fundamental requirements for peaceful co-existence of radar and communication systems is to get rid of the harmful interference signals [7]–[16]. Initially, the spectrum sharing approaches proposed for the co-existence of radar and communication systems address the problem of interference suppression solely at one of the systems, namely either the radar or communication system. Moreover, these works consider only the strategy of transmitting the data of one system in the null space of the interference channel between the two systems, which is typically called null-space projection (NSP). Sodagari *et al.* [11] accomplished the spectrum sharing by working on the radar side. Specifically, they designed the radar waveform to be in the null space of the interference channel between the radar and one-cell communication system. An extension to multi-cell communications scenarios was presented by Khawar *et al.* [12], where the designed radar waveform works in the null space of the interference channel with the largest dimension null space. It is worth to mention that, the system can mitigate interference from only one base station (BS) at any instance of time, which reduces to the one-cell scenario [11]. In [14], a similar approach has been presented but the radar waveform was beamformed to mitigate the interference from all the BSs in the network. Recently, the concept of MIMO radars based on sparse sensing and matrix completion

Manuscript received October 29, 2017; revised April 2, 2018 and July 26, 2018; accepted September 20, 2018. Date of publication October 1, 2018; date of current version December 14, 2018. This work was supported by the National Natural Science Foundation of China under Grants U1713217 and U1501253. The review of this paper was coordinated by Prof. M. Cenk Gursoy. (Corresponding author: Lei Huang.)

M. Rihan is with the Guangdong Key Laboratory of Intelligent Information Processing, College of Information Engineering, Shenzhen University, Shenzhen 518060, China and also with the Department of Electronics and Electrical Communications Engineering, Faculty of Electronic Engineering, Menoufia University, Al-Kawm 21974, Egypt (e-mail: mohamed.elmelegy@el-eng.menofia.edu.eg).

L. Huang is with the Guangdong Key Laboratory of Intelligent Information Processing, College of Information Engineering, Shenzhen University, Shenzhen 518060, China (e-mail: dr.lei.huang@ieee.org).

Color versions of one or more of the figures in this paper are available online at <http://ieeexplore.ieee.org>.

Digital Object Identifier 10.1109/TVT.2018.2872917

has been presented in [7] and [8]. Such a kind of MIMO radar is superior to the other existing categories in terms of reducing both the communication bandwidth and power, as well as the ability to modulate the interference channel from the communication transmitters in an adaptive fashion so as to minimize the interference to the radar under some rate and power constraints. However, the works in [7] and [8] have given much more attention to the radar performance than the communication system performance. Specifically, they considered designing the communication transmit covariance matrix to minimize the effective interference at the radar receiver under capacity and power constraints for the communication system. Accordingly, while the performance of the radar system is optimized in some sense, the communication system is sub-optimal, keeping it only under some performance constraints.

As we have discussed above, interference mitigation is the fundamental issue for peaceful co-existence and effective spectrum sharing concept between wireless systems. Recently, interference alignment (IA) has been proposed as one of the promising solutions to suppress electromagnetic interference in the future interference-limited wireless networks [17]. The key idea of IA is to maximize the dimension of the interference-free subspace at each receiver, which is assigned for useful signal through aligning the interference signals within the subspace of minimum dimension [22]. With the advent of IA, the maximum achievable capacities of various network scenarios were investigated, e.g., MIMO interference channel (MIMO-IC) and MIMO X-channel [23]. Additionally, IA has been employed as the transmission technology for many advanced network architectures, e.g., uplink and downlink cellular networks [24], [25], and small cell and/or heterogeneous networks (HetNets) [26]–[28]. Moreover, IA is also employed for limited feedback designs of many interference-limited networks [29]. However, IA has not yet been considered for mitigating the interference in heterogeneous wireless environments in which radar and communication systems share the same spectrum bands. This motivation opens the door for our proposed approach to tackle interference arising between two of the most important wireless systems, which according to official reports [5], [6], have not yet exploited their spectral resources efficiently.

The challenges of simultaneously managing the interference at both the radar and communication systems lie in the needs of information sharing, channel state information (CSI) feedback, and the security issues in information exchange [15], [16]. If the two systems are aware of the existence of each other, it is possible for them to cooperatively exchange their information to help in optimally designing their transmissions under some security constraints which are desirable for radar as well as communication systems. Actually, the interference management has been addressed in literature of cognitive radio but only from the perspective of communication systems. However, the peaceful coexistence between radar and communication becomes more challenging because the interference signals to be mitigated result not only from communication but also from radar. This motivates us to develop efficient methodologies to tackle such a challenging issue.

In this paper, we propose an optimum co-design of spectrum sharing between the MIMO radar and MIMO communication systems. This proposal targets the performance metrics for both systems, namely signal to interference plus noise ratio (SINR) for MIMO radar and sum-rate for MIMO communication.

Specifically, we propose a two-tier alternative optimization (TTAO) framework for achieving peaceful co-existence of MIMO radar and communication systems with maximum performance for both systems. The TTAO framework consists of the main iterative algorithm with two iterative sub-algorithms, which all based on the alternative optimization technique [30], leading to optimum performance for the two systems. Our main contributions are summarized as follows:

- 1) The problem of spectrum sharing between the MIMO radar and MIMO communication is considered and an IA-based framework, namely TTAO, is suggested to improve the performance of the two wireless systems under spectrum sharing conditions through employing IA as a smart interference mitigation scheme.
- 2) An integrated network architecture for coordinating the spectrum sharing between MIMO radar and cellular communication systems has been proposed. The core of such architecture is the central control unit (CCU), which may be functionally integrated with the radar fusion center that is usually provided with extraordinary computational capability, to perform complex processing tasks. The central unit is responsible for collecting the CSI of both systems as well as compute the transmit and receive beamforming matrices based on the proposed framework.
- 3) The proposed TTAO framework aims to maximize both the SINR at MIMO radar receiver and the average sum-rate of MIMO communication, therefore two optimization problems are derived to manipulate such a design.
- 4) The first tier of the proposed framework consists of two iterative sub-algorithms that utilize an alternative optimization procedure to compute the transmit and receive beamforming matrices for optimal design. The second tier is to consecutively iterate between the two sub-algorithms of the first tier, ending up with a globally iterative approach which is able to provide the optimal trade-off between the SINR for MIMO radar and the average sum-rate for MIMO communication.
- 5) We study the convergence of the whole framework through simulations for both weak and strong interference channels, which reveals that the proposed framework is able to reach a stationary point after some iterations.

The remainder of the paper is organized as follows. Section II introduces the system model when the MIMO radar and MIMO communication systems co-exist. The formulation of spectrum sharing problem between MIMO communication and MIMO radar is investigated in Section III. Numerical results are presented in Section IV. Finally, the paper is concluded in Section V.

Notation: Vectors and matrices are written in boldface lower-case letters and boldface upper-case letters, respectively. The \mathbf{A}^T and \mathbf{A}^\dagger are referred to as the transpose and the complex Hermitian transpose of matrix \mathbf{A} , respectively. The expression $\cos(\mathbf{A})$ or $\sin(\mathbf{A})$, refers to the matrix whose elements are $\cos(\cdot)$ or $\sin(\cdot)$ of the corresponding elements in \mathbf{A} . The expression $\text{diag}(d_1, \dots, d_n)$ denotes the diagonal matrix with d_1, \dots, d_n being the diagonal elements. The symbols $\text{Tr}(\mathbf{A})$, $\|\mathbf{A}\|_2$, $\text{Vec}(\mathbf{A})$, and $\|\mathbf{A}\|_F$ represent the trace, 2– norm, the stacked columns, and Frobenius norm of matrix \mathbf{A} . The matrix \mathbf{I}_n stands for the identity matrix of size $n \times n$, and $\mathbf{0}_d$ is an all-zero matrix of size $d \times d$. The $\mathbf{x} \sim \mathcal{CN}(\mu, \Sigma)$ means that \mathbf{x} is complex Gaussian distributed with mean μ and covariance matrix Σ . The expression $\mathbf{B} = \nu_{\min}^d(\mathbf{A})$ means that matrix \mathbf{B}

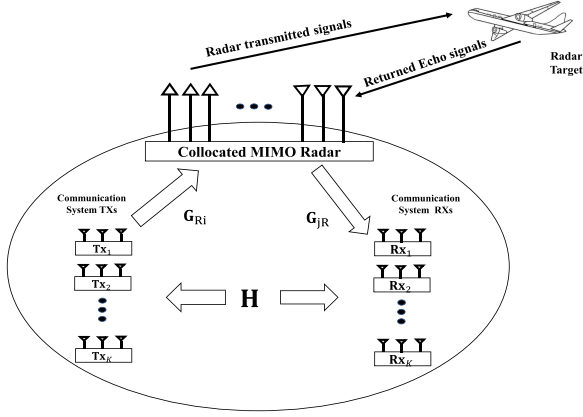


Fig. 1. Spectrum sharing between MIMO communications and collocated MIMO radar. The communication system is assumed as a K -user MIMO interference channel which can be easily modified to the situations of one- or multi-cell communication system.

consists of the eigenvectors corresponding to the smallest d eigenvalues of \mathbf{A} . The expression $\{\mathbf{A} \parallel \mathbf{B}\}$ denotes the horizontal concatenation of the matrices \mathbf{A} and \mathbf{B} . Finally, $\mathbb{E}\{X\}$ refers to the expectation of random variable X .

II. SYSTEM MODEL AND PRELIMINARIES

Consider a MIMO radar system that is in close proximity, and shares the spectrum with a MIMO communication system as shown in Fig. 1. Specifically, we consider a collocated MIMO radar that uses a transmit uniform linear array (ULA) of M_t antennas and a receive ULA of M_r antennas, and the inter-element distances of the transmit and receive ULAs are half-wavelength. Without loss of generality and for easy of mathematical manipulations, we assume that the arrays have the same number of elements, i.e., $M = M_t = M_r$, at both the transmitter and receiver of the MIMO radar system. On the other hand, the communication system consists of K -user pairs MIMO system with N_t and N_r antennas at each transmitter and receiver, respectively. Without loss of generality, we assume that the numbers of transmit and receive antennas for all users are the same; $N = N_t = N_r$. The communication channel between transmitter i and receiver j is denoted as $\mathbf{H}_{ji} \in \mathbb{C}^{N \times N}$. The interference channel from the radar transmitter to the communication receiver j is denoted as $\mathbf{G}_{jR} \in \mathbb{C}^{N \times M}$, and that from a communication transmitter i to radar receiver is referred to as, $\mathbf{G}_{Ri} \in \mathbb{C}^{M \times N}$. It is assumed that all the channels \mathbf{H}_{ji} , \mathbf{G}_{jR} , and \mathbf{G}_{Ri} are block faded, quasi-static and perfectly known at all the transmitters. This assumption can be justified through the employment of the proposed integrated architecture explained at the end of this section. Specifically, this can be realized through either a cooperative backhaul connection or the transmission of pilot signals between the two systems to estimate and exchange the CSI. Moreover, we assume a perfect carrier phase synchronization between the two systems [32].

Let the discrete time baseband signal transmitted by the radar transmit array is expressed as $\mathbf{s}(n)$, where n is the time index. Assume that d is the number of samples/streams to be transmitted through the radar such that $d \in \{1, \dots, M\}$. Actually, the MIMO radar is able to provide more degrees-of-freedom than the phased array radar because the former adopts the orthogonal

waveforms. This, in turn, means that the MIMO radar needs to transmit d streams at the same time for target detection. Then the MIMO radar transmit waveform matrix is given as:

$$\mathbf{s}(n) = \sqrt{p_R} [s_1(n) s_2(n) \dots s_d(n)]^T, \in \mathbb{C}^d \quad (1)$$

where $s_i(n) \forall i \in \{1, 2, \dots, d\}$ is the i^{th} pulse of the radar baseband signal. Moreover, p_R is the transmitting power of the MIMO radar. The baseband signal is first precoded by matrix $\mathbf{V} \in \mathbb{C}^{M \times d}$, then transmitted towards a group of L targets with known directions θ_l . At each time instant n , the target echoes and the communication interference signals received at the MIMO radar receiver are decoded using decoding matrix $\mathbf{U} \in \mathbb{C}^{d \times M}$. Based on the Swerling II target model [35], [36], the baseband signal at the radar receiver is given by:

$$\begin{aligned} \mathbf{y}_R(n) = & \sqrt{p_R} e^{-j\omega_D n} \left(\sum_{l=1}^L \alpha_l \mathbf{a}_r(\theta_l) \mathbf{a}_t^\dagger(\theta_l) \right) \mathbf{V} \mathbf{s}(n - n_k) \\ & + \sqrt{p_C} \sum_{i=1}^K \mathbf{G}_{Ri} \mathbf{F}_i \mathbf{x}_i(n) + \mathbf{n}_R(n). \end{aligned} \quad (2)$$

The first term on the right hand side (RHS) of (2) represents the returned echo signals from the radar targets. On the other hand, the second term on the RHS represents the interference signals received from the communication transmitters. The $\mathbf{y}_R(n) \in \mathbb{C}^d$ refers to the radar received signal. The term $e^{-j\omega_D n}$ expresses the Doppler frequency shift for the returned echos. Additionally, the $\mathbf{x}_i(n) \in \mathbb{C}^d$ is denoting the signal transmitted from the communication transmitter i , and it satisfies $\mathbb{E}\{\|\mathbf{x}_i\|^2\} = 1$. The maximum transmission power of each communication transmitter is set to p_C . These communication signals are first precoded using the precoding matrices $\mathbf{F}_i \forall i \in \{1, 2, \dots, K\}$, before transmission. The symbols n_k , and ω_D denote the sum of the propagation delays to and from the target and the Doppler frequency shift, respectively. The term $\mathbf{n}_R(n)$ is the independent identically distributed (i.i.d.) complex Gaussian random process with zero mean and covariance matrix $\sigma_R^2 \mathbf{I}_M$. The symbol α_l is the complex path loss that includes the coefficient of the reflection, the propagation loss, and the complex radar cross section of the target, which is assumed to be a complex Gaussian distributed with mean zero and variance $\sigma_{\alpha_l}^2$. The vectors $\mathbf{a}_t(\theta_l)$ and $\mathbf{a}_r(\theta_l)$ stand for the transmit and receive steering vectors for target l , respectively. The transmit steering vector, with equal inter-element spacing of half wavelength, can be defined as:

$$\mathbf{a}_t(\theta_l) \triangleq [1 e^{-j\pi \sin(\theta_l)} e^{-j2\pi \sin(\theta_l)} \dots e^{-j(M-1)\pi \sin(\theta_l)}], \quad (3)$$

Since, $M = M_t = M_r$, we have, $\mathbf{a}(\theta) \triangleq \mathbf{a}_t(\theta) \triangleq \mathbf{a}_r(\theta)$. Then, the transmit-receive steering matrix can be written as:

$$\mathbf{A}(\theta_l) \triangleq \mathbf{a}_r(\theta_l) \mathbf{a}_t^\dagger(\theta_l) \triangleq \mathbf{a}(\theta_l) \mathbf{a}^\dagger(\theta_l). \quad (4)$$

In order to keep the system model tractable, the following assumptions are needed [35], [36]:

- Due to the far-field implementations, the path loss factor, α_l , can be assumed identical for all transmit and receive antenna elements.
- The angle θ_l stands for the azimuth angle of the target.

Based on the above assumptions together with range-Doppler compensation [35], (2) can be rewritten as:

$$\mathbf{y}_R(n) = \sqrt{p_R} \left(\sum_{l=1}^L \alpha_l \mathbf{A}(\theta_l) \right) \mathbf{V} \mathbf{s}(n) + \sqrt{p_C} \sum_{i=1}^K \mathbf{G}_{Ri} \mathbf{F}_i \mathbf{x}_i(n) + \mathbf{n}_R(n). \quad (5)$$

After decoding the received signal at the radar receiver, the resulting signal can be expressed as:

$$\mathbf{U}^\dagger \mathbf{y}_R(n) = \sqrt{p_R} \mathbf{U}^\dagger \left(\sum_{l=1}^L \alpha_l \mathbf{A}(\theta_l) \right) \mathbf{V} \mathbf{s}(n) + \sqrt{p_C} \mathbf{U}^\dagger \sum_{i=1}^K \mathbf{G}_{Ri} \mathbf{F}_i \mathbf{x}_i(n) + \mathbf{U}^\dagger \mathbf{n}_R(n). \quad (6)$$

We assume that the MIMO communication system uses the same carrier frequency as the MIMO radar, and both systems sample their baseband signals at the same sampling rate. The discrete time communication signal at receiver j has the following form:

$$\mathbf{y}_{j,C}(n) = \sqrt{p_C} \sum_{i=1}^K \mathbf{H}_{ji} \mathbf{F}_i \mathbf{x}_i(n) + \sqrt{p_R} \mathbf{G}_{jR} \mathbf{V} \mathbf{s}(n) + \mathbf{n}_c(n). \quad (7)$$

Here, $\mathbf{n}_c(n)$ denotes the additive white noise with complex Gaussian distribution $\mathcal{CN}(0, \sigma_c^2)$ at receiver j . Here, σ_c^2 denotes the noise variance at receiver j in the communication system. The first term on the RHS of (7) includes both the desired communication signal, i.e., $\mathbf{H}_{ji} \mathbf{F}_i \mathbf{x}_i(n)$, and the inter-user interference signal, i.e., $\sum_{i \neq j}^K \mathbf{H}_{ji} \mathbf{F}_i \mathbf{x}_i(n)$. Each communication receiver j uses a decoding matrix \mathbf{W}_j to separate the useful signals from the interference signals, given as:

$$\mathbf{W}_j^\dagger \mathbf{y}_{j,C}(n) = \sqrt{p_C} \mathbf{W}_j^\dagger \sum_{i=1}^K \mathbf{H}_{ji} \mathbf{F}_i \mathbf{x}_i(n) + \sqrt{p_R} \mathbf{W}_j^\dagger \mathbf{G}_{jR} \mathbf{V} \mathbf{s}(n) + \mathbf{W}_j^\dagger \mathbf{n}_c(n). \quad (8)$$

The following assumptions are made regarding the proposed framework and the proposed radar-communication integrated network architecture:

- 1) We assume that the MIMO radar and MIMO communication systems are integrated through implementing a central control unit (CCU) in order to guarantee the full coordination between the two systems as shown in Fig. 2. This CCU can be functionally integrated with the radar fusion center in order to guarantee the security of radar data. Usually, the fusion center of the radar is used to accomplish the complex processing tasks that need huge computational capabilities. Accordingly, the proposed CCU is also assumed to own extra-high computational capabilities to accomplish the ordinary fusion center tasks as well as the task needed to execute the proposed spectrum sharing framework. The CCU is responsible for collecting the CSI of the communication system, namely, \mathbf{H} as well as the MIMO radar parameters, namely, $\{\mathbf{G}_{Ri}, \mathbf{G}_{jR}, \mathbf{C}\}$. Then it uses the proposed framework to compute the transmit and receive beamforming filters based on IA. Finally, it distributes these filters to its corresponding systems.

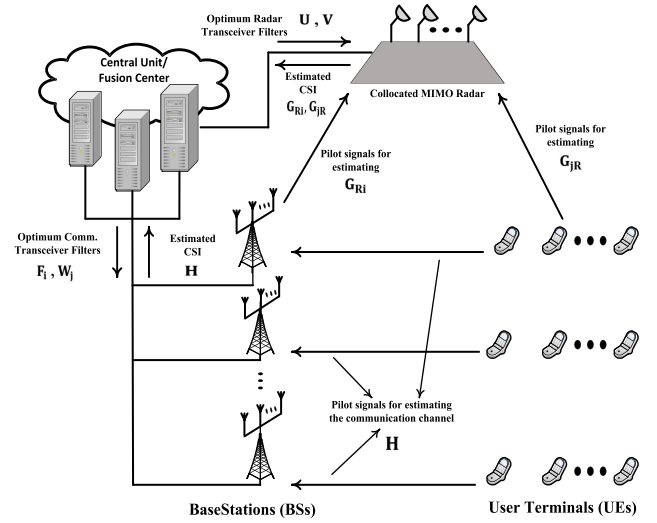


Fig. 2. The integrated system architecture of the proposed spectrum sharing framework. The proposed co-design is performed in central manner at the central unit which can be integrated with the radar fusion center for privacy issues related to radar data.

- 2) Performing the co-design centrally protects the network from the overwhelming CSI exchange as well as saving both the radar and the communication systems from excessive computations.
- 3) We assume the channel \mathbf{H} is perfectly known at the communication transmitters, mostly BSs, and the inter-systems interference channels \mathbf{G}_{Ri} and \mathbf{G}_{jR} are assumed to be perfectly known at the radar. These assumptions can be considered feasible by using pilot signal-based CSI estimation [7]–[12]. The CCU can efficiently coordinate the transmission of pilot signals between the two systems, assuming the systems are operated in TDD fashion to support channel reciprocity. For example, each communication transmitter i transmits a pilot signal to the radar in order to estimate its corresponding channel \mathbf{G}_{Ri} . Additionally, each communication receiver j transmits pilot signals to both the radar and the communication BSs in order to estimate the \mathbf{G}_{jR} and \mathbf{H} , respectively. All the estimation processes depend on channel reciprocity [13]. Finally, the CSI estimates are forwarded to the central unit through the MIMO radar and the communication BSs.
- 4) The two systems can work at different sampling rates as assumed in [7]. However, for facilitating the coordination between the two systems, we assume that the two systems transmit narrowband waveforms with the same sampling rate or the same symbol period. In order to test the feasibility for the MIMO radar and MIMO communication systems to work with the same sampling rate, let us assume an S-band MIMO radar with range resolution 300 m, which is typically between 100 m and 600 m [8]–[9]. Accordingly, the radar sub-pulse duration is 2μ seconds. On the other side, the typical symbol duration in modern cellular communications is also 2μ seconds [10]. This justifies the use of equal sampling rate for the two systems, say, 0.5×10^6 symbols/sec.
- 5) The process of the proposed framework consists of two phases, namely, the training/feedback and operation phases. During the training/feedback phase, the CCU

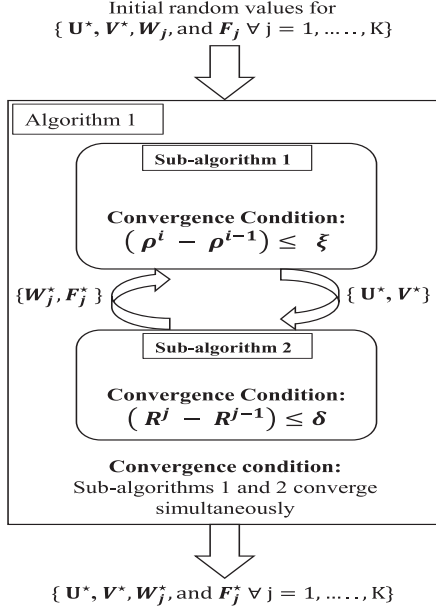


Fig. 3. The proposed algorithm with its sub-algorithms which constitute the spectrum sharing framework and how they interact with one another. The parameters ξ and δ are the decision variables for Sub-algorithms 1 and 2, respectively.

acquires receivers' CSI through training sequences or pilots, then shares them with the transmitters via feedback. Accordingly, the transceiver pairs use the obtained CSI to evaluate the optimal IA-based transceivers' beamformers. During the operation phase, the co-designed beamformers are used to carry out the framework and achieve the peaceful coexistence between radar and communication.

III. INTERFERENCE ALIGNMENT BASED SPECTRUM SHARING DESIGN

In this section, we present an IA based framework for spectrum sharing between the MIMO radar and MIMO communication systems. The proposed framework consists of a main algorithm with two underlying sub-algorithms, which are jointly used to maximize the SINR for the radar system and the sum-rate/throughput of the communication system. Fig. 3 shows how the main algorithm and its sub-algorithms interact with each other to accomplish the aims of the proposed framework. Since the main performance metrics for both systems are directly related to mitigating the mutual interference arising when the two systems are working in close proximity to each other, the IA approach is tailored to tackle the issue of interference suppression in the co-existence design of MIMO radar and MIMO communications. To this end, the proposed framework is able to provide the optimal design of the transmit precoders and receive spatial filters (\mathbf{U} , \mathbf{V} , \mathbf{W}_i , and \mathbf{F}_i ; $i = 1, \dots, K$) in the sense that the following requirements are met:

- 1) $\mathbf{W}_j^\dagger \mathbf{G}_{jR} \mathbf{V} = \mathbf{0}_d$,
- 2) $\mathbf{U}^\dagger \sum_{i=1}^K \mathbf{G}_{Ri} \mathbf{F}_i = \mathbf{0}_d$,
- 3) $\text{Rank}(\mathbf{W}_j^\dagger \sum_{i=1}^K \mathbf{H}_{ji} \mathbf{F}_i) = d$,
- 4) Maximum SINR at the radar receiver.

The first equality above guarantees that the radar interference signals at the communication receivers are aligned to a

subspace, optimally, with zero dimensions. The second equality means that the communication interference signals at the radar receiver are aligned to a subspace, optimally, with zero dimensions. Note that if the channel coefficients are independently drawn from a continuous distribution and the channel matrices have no special structure, the third and fourth requirements would be satisfied almost surely provided that the second equality could be satisfied. Accordingly, the feasibility of the proposed framework reflected by the above conditions can be considered as the typical feasibility conditions for applying IA in MIMO interference channels [22]–[24].

The performance metric for radar that has been commonly used in waveform design is the SINR, which reflects the strength of the returned echo signals with respect to the noise and interference signals, and accordingly the probability of detection of the targets. The echos returned from all the targets have covariance matrix $\mathbb{E} \{ \mathbf{U}^\dagger \mathbf{C} \mathbf{V} \mathbf{s}(n) \mathbf{s}^\dagger(n) \mathbf{V}^\dagger \mathbf{C}^\dagger \mathbf{U} \} = p_R \mathbf{U}^\dagger \mathbf{C} \mathbf{V} \mathbf{V}^\dagger \mathbf{C}^\dagger \mathbf{U}$ with $\mathbf{C} = \sum_{l=1}^L \alpha_l \mathbf{A}(\theta_l)$. If the matrices \mathbf{V} , \mathbf{U} , and \mathbf{F}_i are expressed in terms of their column vectors respectively as $[\mathbf{v}_1 \mathbf{v}_2 \dots \mathbf{v}_d]$, $[\mathbf{u}_1 \mathbf{u}_2 \dots \mathbf{u}_d]$, and $[\mathbf{f}_{i1} \mathbf{f}_{i2} \dots \mathbf{f}_{id}]$. So, the overall SINR, namely ρ , at the MIMO radar receiver is defined as the sum of the SINR contributions by different pulses or streams received at the MIMO radar receiver. This can be expressed as:

$$\rho = \sum_{r=1}^d \rho_r = \sum_{r=1}^d \frac{\frac{p_R}{d} \mathbf{u}_r^\dagger \mathbf{C} \mathbf{v}_r \mathbf{v}_r^\dagger \mathbf{C}^\dagger \mathbf{u}_r}{\frac{p_C}{d} \mathbf{u}_r^\dagger \left(\sum_{i=1}^K \mathbf{G}_{Ri} \mathbf{f}_{ir} \mathbf{f}_{ir}^\dagger \mathbf{G}_{Ri}^\dagger \right) \mathbf{u}_r + \sigma_R^2 \mathbf{u}_r^\dagger \mathbf{u}_r}. \quad (9)$$

Assuming that the radar knows the target directions, i.e., the matrix \mathbf{C} is known, so the problem of maximizing the overall SINR ρ at the radar receiver, can be formulated as:

$$(\mathbf{P}_1) \quad \max_{\mathbf{V}, \mathbf{F}_i, \mathbf{U}, \mathbf{W}_i} \rho$$

subject to $\mathbf{V}^\dagger \mathbf{V} = \mathbf{I}_d$. (10)

Assuming that the feasibility conditions for IA are held for the proposed scenario [17], the design problem at the MIMO communication side is to maximize the total sum-rate of the communication network. Accordingly, this can be mathematically formulated as the optimization problem \mathbf{P}_2 .

$$(\mathbf{P}_2) \quad \max_{\mathbf{V}, \mathbf{F}_j, \mathbf{U}, \mathbf{W}_j} \sum_{j=1}^K \log_2 \left| \mathbf{I} + \frac{p_C \mathbf{W}_j^\dagger \mathbf{H}_{jj} \mathbf{F}_j \mathbf{F}_j^\dagger \mathbf{H}_{jj}^\dagger \mathbf{W}_j}{\mathbf{W}_j^\dagger \mathbf{B}_j \mathbf{W}_j} \right|$$

subject to

$$\mathbf{W}_j^\dagger \mathbf{G}_{jR} \mathbf{V} = \mathbf{0}_d,$$

$$\mathbf{U}^\dagger \sum_{i=1}^K \mathbf{G}_{Ri} \mathbf{F}_i = \mathbf{0}_d,$$

$$\mathbf{W}_j^\dagger \sum_{i=1}^K \mathbf{H}_{ji} \mathbf{F}_i = \mathbf{0}_d,$$

$$\mathbf{V}^\dagger \mathbf{V} = \mathbf{I}_d \text{ \& } \mathbf{W}_j^\dagger \mathbf{W}_j = \mathbf{I}_d, \quad \forall j = 1, \dots, K$$

$$\mathbf{F}_i^\dagger \mathbf{F}_i = \mathbf{I}_d \text{ \& } \mathbf{U}^\dagger \mathbf{U} = \mathbf{I}_d, \quad \forall i = 1, \dots, K; i \neq j$$

$$\mathbf{W}_j^\dagger \mathbf{H}_{ji} \mathbf{F}_i = \mathbf{0}_d, \quad \forall i, j = 1, \dots, K; i \neq j \quad (11)$$

Sub-algorithm 1: Max-SINR Based Iterative Transmit-Receive Beamforming Design for MIMO-Radar.

- 1: **Initialization:** σ_n^2, ξ , and $\mathbf{F}_i, \forall i \in \{1, 2, \dots, K\}$, which is initialized by constant beamformers randomly or evaluated and feedback from Sub-algorithm 2, let the iteration index $t_1 = 1$;
 - 2: **while** $(\rho^{t_1} - \rho^{t_1-1}) \leq \xi$ **do**
 - 3: Randomly initiate the transmit beamforming matrix for the MIMO radar \mathbf{V} .
 - 4: Compute the interference plus noise covariance matrix, \mathbf{B}_{RC} , at receiver i using (14).
 - 5: Compute the radar optimal receive beamforming matrix, $\mathbf{U} = [\mathbf{u}_1 \mathbf{u}_2 \dots \mathbf{u}_d]$, for the current iteration using (15).
 - 6: Compute the ρ^{t_1-1} , based on the obtained \mathbf{U} using (9).
 - 7: Compute interference plus noise covariance matrix for the reverse communication direction, \mathbf{R}_{CR} using (17).
 - 8: Compute the radar optimal transmit beamforming matrix, $\mathbf{V} = [\mathbf{v}_1 \mathbf{v}_2 \dots \mathbf{v}_d]$, of the current iteration using (16).
 - 9: Normalize the optimal \mathbf{V} ; to keep $\mathbf{V}^\dagger \mathbf{V} = \mathbf{I}_d$.
 - 10: Compute the ρ^{t_1} , based on the updated \mathbf{V} using (9).
 - 11: Update the iteration index to $t_1 + 1$.
 - 12: **end while**
 - 13: **Output:** The optimal solution $\{\mathbf{U}^*, \mathbf{V}^*\}$
-

where, \mathbf{B}_j is the interference plus noise covariance matrix at receiver j , given by:

$$\mathbf{B}_j = p_C \sum_{\substack{j=1 \\ j \neq i}}^K \mathbf{H}_{ji} \mathbf{F}_i \mathbf{F}_i^\dagger \mathbf{H}_{ji}^\dagger + p_R \mathbf{G}_{jR} \mathbf{V} \mathbf{V}^\dagger \mathbf{G}_{jR}^\dagger + \sigma_c^2 \mathbf{I}_N. \quad (12)$$

A. Transceiver Design for MIMO Radar System

The most important performance criteria for MIMO radars is the SINR which corresponds to the probability of detection. In this subsection, an iterative alternating optimization (AO) based sub-algorithm, similar in concept to [18]–[20], is used to solve (10), ending up with optimal designs of the transmit precoder and receive spatial filter in the MIMO radar. In this sub-algorithm, \mathbf{V} and \mathbf{U} are alternatively optimized, while the other variables are kept unchanged, whose values are forwarded from Sub-algorithm 2. Mathematically speaking, the optimization problem \mathbf{P}_1 is solved for \mathbf{U} while \mathbf{V} is fixed and vice versa. This iteration is not terminated until a convergence criterion is met. During each iteration the optimum beamforming matrices \mathbf{F}_i are forwarded from Sub-algorithm 2 and used as constant for all the iterations of Sub-algorithm 1. In the first part of the design process, we solve the $\{\mathbf{P}_1\}$ for optimum \mathbf{U} with \mathbf{V} kept fixed. The optimization problem in (10) can be rewritten as:

$$\begin{aligned} (\mathbf{P}_{1.1}) \quad & \max_{\mathbf{U}=[\mathbf{u}_1 \mathbf{u}_2 \dots \mathbf{u}_d]} \sum_{r=1}^d \frac{\mathbf{u}_r^\dagger \mathbf{C} \mathbf{v}_r \mathbf{v}_r^\dagger \mathbf{C}^\dagger \mathbf{u}_r}{\mathbf{u}_r^\dagger \mathbf{B}_{RC} \mathbf{u}_r}, \\ & \text{s.t. } \mathbf{V}^\dagger \mathbf{V} = \mathbf{I}_d \end{aligned} \quad (13)$$

Sub-algorithm 2: Interference Alignment Based Transmit-Receive Beamforming Design for MIMO Communication.

- 1: **Initialization:** σ_C^2, d (the issued DoFs for each user), δ the decision parameter of the algorithm, and \mathbf{V} , which is forwarded from Sub-algorithm 1, let the iteration index $t_2 = 1$;
- 2: **while** $(\mathcal{R}_{sum}^{t_2} - \mathcal{R}_{sum}^{t_2-1}) \leq \delta$ **do**
- 3: Randomly initiate the set of transmit beamformers \mathbf{F}_i .
- 4: Evaluate the interference covariance matrices at the receivers by using:

$$\mathbf{Q}_j = \left\{ \left[\sum_{\substack{i=1 \\ i \neq j}}^K \underbrace{\mathbf{H}_{ji} \mathbf{F}_i \mathbf{F}_i^\dagger \mathbf{H}_{ji}^\dagger}_{\mathbf{Q}_{ji}} \right] \left[\underbrace{\mathbf{G}_{jR} \mathbf{V} \mathbf{V}^\dagger \mathbf{G}_{jR}^\dagger}_{\mathbf{Q}_{jR}} \right] \right\}.$$

- 5: Compute the receive beamformers that minimize the leakage interference as:

$$\mathbf{W}_j = \nu_{\min}^d(\mathbf{Q}_j).$$
- 6: Compute the gradient matrix of the sum-rate with respect to \mathbf{W}_j using (27).
- 7: Compute the singular value decomposition of the gradient matrix as in (28).
- 8: Compute the updated value of the receive beamformer using (29) with replacing the \mathbf{F}_j by \mathbf{W}_j , where the step size is given an initial value, $\Delta_0 = 0.1$, then it is calculated from the relation $\Delta_{t_2+1} = 0.995 \Delta_{t_2}$.
- 9: Compute the updated transmit beamformers by performing the steps from (3) to (8) with exchanging the roles of the transmit and receive beamformers and using the covariance matrices for the reciprocal channels as:

$$\mathbf{Q}_j = \left\{ \left[\sum_{\substack{i=1 \\ i \neq j}}^K \underbrace{\mathbf{H}_{ji}^\dagger \mathbf{W}_i \mathbf{W}_i^\dagger \mathbf{H}_{ji}}_{\mathbf{Q}_{ji}} \right] \left[\underbrace{\mathbf{G}_{jR}^\dagger \mathbf{U} \mathbf{U}^\dagger \mathbf{G}_{jR}}_{\mathbf{Q}_{jR}} \right] \right\}.$$

- 10: Compute the updated value for $\mathcal{R}_{sum}^{t_2}$ through:

$$\mathcal{R}_{sum}^{t_2} = \sum_{j=1}^K \log_2 \left| \mathbf{I}_N + \left(p_C \sum_{i=1}^K \mathbf{Q}_{ji} + p_R \mathbf{Q}_{jR} + \sigma_C^2 \mathbf{I}_N \right)^{-1} (p_C \mathbf{Q}_{jj}) \right|$$

- 11: Update the iteration index to $t_2 + 1$.
 - 12: **end while**
 - 13: **Output:** The optimum solution $\{\mathbf{W}_j^*, \mathbf{F}_j^*\}$.
-

where

$$\mathbf{B}_{RC} = \frac{p_C}{d} \left(\sum_{i=1}^K \sum_{r=1}^d \mathbf{G}_{Ri} \mathbf{f}_{ir} \mathbf{f}_{ir}^\dagger \mathbf{G}_{Ri}^\dagger \right) + \sigma_R^2 \mathbf{I}_M. \quad (14)$$

Following the same strategy in [22] to solve (13), so, the unit vector \mathbf{u}_r^* that maximizes the SINR corresponding to the column

r , is given by:

$$\mathbf{u}_r^* = \frac{\mathbf{B}_{RC}^{-1} \mathbf{C} \mathbf{v}_r}{\|\mathbf{B}_{RC}^{-1} \mathbf{C} \mathbf{v}_r\|_2}. \quad (15)$$

where $\mathbf{U}^* = [\mathbf{u}_1^*, \mathbf{u}_2^*, \dots, \mathbf{u}_d^*]$ is the optimal receive beamforming matrix for the MIMO radar receiver. In the second part of the design process, we fix the receive beamforming matrix \mathbf{U} , and optimize the transmitted waveform \mathbf{V} using a similar fashion. Accordingly, the unit vector \mathbf{v}_r^* that maximizes the SINR in the reverse direction is given by:

$$\mathbf{v}_r^* = \frac{\mathbf{B}_{CR}^{-1} \mathbf{C}^\dagger \mathbf{u}_r^*}{\|\mathbf{B}_{CR}^{-1} \mathbf{C}^\dagger \mathbf{u}_r^*\|_2}, \quad (16)$$

where

$$\mathbf{B}_{CR} = \frac{p_C}{d} \left(\sum_{j=1}^K \sum_{r=1}^d \mathbf{G}_{jR} \mathbf{W}_{jr} \mathbf{W}_{jr}^\dagger \mathbf{G}_{jR}^\dagger \right) + \sigma_R^2 \cdot \mathbf{I}_M. \quad (17)$$

The whole iterative optimization procedures used to obtain the optimal transmit and receive beamformers for the MIMO radar systems are summarize in Sub-algorithm 1.

B. Transceiver Design for MIMO Communication System

The sub-algorithm proposed in this subsection aims to maximize the sum-rate of the MIMO communication network by alternatively optimizing the transmit and receive beamforming filters based on the principle of IA. Alternative optimization approach is used heavily in the context of IA for different MIMO interference channels [22]–[25]. For ease of manipulation, the covariance matrix for the interference between users i and j in the communication system and the radar system can be expressed, respectively, as:

$$\mathbf{Q}_{ji} = \mathbf{H}_{ji} \mathbf{F}_i \mathbf{F}_i^\dagger \mathbf{H}_{ji}^\dagger, \text{ \& } \mathbf{Q}_{jR} = \mathbf{G}_{jR} \mathbf{V} \mathbf{V}^\dagger \mathbf{G}_{jR}^\dagger. \quad (18)$$

For the reciprocal channels, where the roles of the transmit and receive beamforming matrices are interchanged, they can be expressed, respectively, as:

$$\mathbf{Q}_{ij} = \mathbf{H}_{ji}^\dagger \mathbf{W}_i \mathbf{W}_i^\dagger \mathbf{H}_{ji}, \text{ \& } \mathbf{Q}_{Rj} = \mathbf{G}_{jR}^\dagger \mathbf{U} \mathbf{U}^\dagger \mathbf{G}_{jR}. \quad (19)$$

Since the interference can be more easily manipulated using the notation of the leakage interference power, so the first three constraints in (11) can be reformulated as:

$$\mathbb{C}_1 : \left\| \mathbf{W}_j^\dagger \mathbf{G}_{jR} \mathbf{V} \mathbf{V}^\dagger \mathbf{G}_{jR}^\dagger \mathbf{W}_j \right\|_F = 0, \forall j = 1, \dots, K. \quad (20)$$

$$\mathbb{C}_2 : \left\| \sum_{i=1}^K \mathbf{U}^\dagger \mathbf{G}_{Ri} \mathbf{F}_i \mathbf{F}_i^\dagger \mathbf{G}_{Ri}^\dagger \mathbf{U} \right\|_F = 0, \forall i = 1, \dots, K. \quad (21)$$

$$\mathbb{C}_3 : \left\| \sum_{i=1}^K \sum_{\substack{j=1 \\ j \neq i}}^K \mathbf{W}_j^\dagger \mathbf{H}_{ji} \mathbf{F}_i \mathbf{F}_i^\dagger \mathbf{H}_{ji}^\dagger \mathbf{W}_j \right\|_F = 0, \forall i, j = 1, \dots, K. \quad (22)$$

Based on (18), (19), (20), (21), and (22), the optimization problem (\mathbf{P}_2) can be written as:

$$\begin{aligned} (\mathbf{P}_2) \max_{\mathbf{F}_j, \mathbf{W}_j} & \sum_{j=1}^K \log_2 \left| \mathbf{I}_N \right. \\ & \left. + \left(p_C \sum_{i=1}^K \mathbf{Q}_{ji} + p_R \mathbf{Q}_{jR} + \sigma_C^2 \mathbf{I}_N \right)^{-1} (p_C \mathbf{Q}_{jj}) \right| \\ \text{subject to} & \\ & \mathbb{C}_1, \mathbb{C}_2, \mathbb{C}_3, \\ & \mathbf{F}_j^\dagger \mathbf{F}_j = \mathbf{I}_d, \quad \mathbf{W}_j^\dagger \mathbf{W}_j = \mathbf{I}_d, \quad \forall i, j = 1, \dots, K \\ & \mathbf{F}_R^\dagger \mathbf{F}_R = \mathbf{I}_d, \quad \mathbf{W}_R^\dagger \mathbf{W}_R = \mathbf{I}_d. \end{aligned} \quad (23)$$

Note that the variables of the above optimization problem are only the transmit and receive beamformers, \mathbf{F}_i and $\mathbf{W}_i \forall i \in \{1, \dots, K\}$, and the optimal values of the transmit and receive beamformers of the radar system are determined by Sub-algorithm 1.

In order to achieve the maximum sum-rate based on IA, the proposed sub-algorithm will apply a combination of the gradient descent and the AO approaches. Using AO, the proposed sub-algorithm alternatively optimize the sum-rate of the communication system with respect to the transmit or receive beamforming matrices while keeping other parameters unchanged. Additionally, the movement of the obtained solution from one iteration to the next will be in the direction of the gradient of the sum-rate function, namely the cost function in (23), with respect to either the transmit or receive beamforming matrices and belong.

To solve the optimization problem \mathbf{P}_2 in (23) in an iterative fashion, we first compute the gradient of the sum-rate function of the communication system, denotes as \mathcal{R}_{sum} , with respect to \mathbf{F}_j through using (18), or with respect to \mathbf{W}_j through using (19). These gradients can be obtained utilizing a similar technique to that employed in [21]. Then, the gradient of the sum-rate with respect to \mathbf{F}_j^\dagger can be calculated as:

$$\begin{aligned} \nabla_{\mathbf{F}_j} \mathcal{R}_{sum} &= \sum_{i=0}^K \left(\mathbf{H}_{ij} \Phi_i^{-1} \mathbf{H}_{ij} - \text{Tr} \left(\mathbf{F}_j^\dagger \mathbf{H}_{ij} \Phi_i^{-1} \mathbf{H}_{ij} \mathbf{F}_j \right) \right) \mathbf{F}_j \\ &+ \sum_{\substack{i=1 \\ i \neq j}}^K \left(\text{Tr} \left(\mathbf{F}_j^\dagger \mathbf{H}_{ij} \Pi_i^{-1} \mathbf{H}_{ij} \mathbf{F}_j \right) - \mathbf{H}_{ij} \Pi_i^{-1} \mathbf{H}_{ij} \right) \mathbf{F}_j, \end{aligned} \quad (24)$$

where

$$\Phi_i = \sum_{j=1}^K \beta_j \mathbf{H}_{ij} \tilde{\mathbf{F}}_j \tilde{\mathbf{F}}_j^\dagger \mathbf{H}_{ij}^\dagger + p_R \mathbf{G}_{iR} \mathbf{V}_i \mathbf{V}_i^\dagger \mathbf{G}_{iR}^\dagger + \sigma_C^2 \mathbf{I}, \quad (25)$$

$$\Pi_i = \sum_{j \neq i}^K \beta_j \mathbf{H}_{ij} \tilde{\mathbf{F}}_j \tilde{\mathbf{F}}_j^\dagger \mathbf{H}_{ij}^\dagger + p_R \mathbf{G}_{iR} \mathbf{V}_i \mathbf{V}_i^\dagger \mathbf{G}_{iR}^\dagger + \sigma_C^2 \mathbf{I}, \quad (26)$$

with $\mathbf{F}_j = \sqrt{\beta_j} \tilde{\mathbf{F}}_j$ and $\beta_j = p_C / \text{Tr}(\tilde{\mathbf{F}}_j^\dagger \tilde{\mathbf{F}}_j)$. A more detailed derivation of (24) is presented in Appendix A.

Similarly, the gradient expression with respect to \mathbf{W}_i^* can be obtained by replacing each MIMO channel with its reciprocal

and the transmit beamforming matrices with the corresponding receive beamforming matrices in (24). Additionally, in order to obtain the receive beamforming matrices, the covariance matrices in (18) are used instead of those in (19).

In this section, we are seeking for an IA solution that maximizes the sum-rate of the MIMO communication system and, at the same time, forces the interference leakage to the communication signal subspaces to approach zero. This problem can be easily solved as the optimization is performed on the Grassmann manifold [33]. Accordingly, if the unconstrained gradient of the sum-rate with respect to the j^{th} transmit beamformer is $\nabla_{\mathbf{F}_j} \mathcal{R}_{sum}$, then the gradient matrix, which consists of a group of tangent vectors on the Grassmann manifold, is given as [34, Corollary]:

$$\nabla_{\mathbf{F}_j}^{\text{Gr}} \mathcal{R}_{sum} = (\mathbf{I}_N - \mathbf{W}_j \mathbf{W}_j^\dagger) \nabla_{\mathbf{F}_j} \mathcal{R}_{sum}. \quad (27)$$

Performing the singular value decomposition to this gradient matrix, we have:

$$\nabla_{\mathbf{F}_j}^{\text{Gr}} \mathcal{R}_{sum} = \mathbf{Z} \Sigma \mathbf{D}^\dagger. \quad (28)$$

The solution obtained at each step of the alternating minimization approach is moved following the geodesic on the Grassmann manifold according to [34, Th. 2.3], yielding:

$$\mathbf{W}_j^{t+1} = (\mathbf{W}_j^t \mathbf{D} \mathbf{Z}) \begin{pmatrix} \cos(\Sigma \Delta) \\ \sin(\Sigma \Delta) \end{pmatrix} \mathbf{D}^\dagger \quad (29)$$

where the superscript t represents the index of iteration of Sub-algorithm 2, and Δ is the step size of the TTAO approach. It determines the distance moved along the geodesic of the Grassmann Manifold at each iteration. In order to converge to a perfectly aligned solution, this step size must be iteratively decreased and eventually approaches zero. The details of the proposed sum-rate based IA approach is summarized in Sub-algorithm 2.

C. Shared Spectrum Co-Existence Between MIMO Radar and MIMO Communication

In the previous subsections, we have proposed two sub-algorithms for designing the transmit and receive beamforming matrices for both the MIMO radar and the MIMO communication systems. In this subsection, we explain how can these two sub-algorithms be employed in order to achieve the optimum performance for both systems when sharing the same spectrum band. The proposed shared spectrum approach is based on the proposed Sub-algorithms 1, and 2. The proposed algorithm will evolve in iterative fashion by alternatively projecting the obtained solution from Sub-algorithm 1/Sub-algorithm 2 onto the solution space of Sub-algorithm 2/Sub-algorithm 1 and continue repeating this operation until convergence occurs. By the end of this procedures, the proposed framework eventually obtains the optimal beamforming solution that maximizes the figure of merits for both systems. In other words, the obtained optimal values for the transmit and receive beamforming matrices of the MIMO radar and the MIMO communication nodes certainly are able to achieve the maximum SINR at the MIMO radar receiver and the maximum sum-rate performance for the MIMO communication network. The main iterative algorithm that manage the whole process is listed in Algorithm 1. We called it TTAO as both Sub-algorithm 1 and 2 are based on AO between the transmit and receive beamformers for the radar and communication

Algorithm 1: TTAO Approach for Shared Spectrum Co-existence.

- 1: **Initialization:** \mathbf{H}_{ji} , \mathbf{G}_{jR} , and \mathbf{G}_{Ri} , $\forall i$, and $j = 1, 2, \dots, K$, let the iteration index is $t = 1$;
 - 2: **while** missing convergence over the outer tier, **do**
 - 3: Compute the transmit and receive beamformers, \mathbf{V}^t and \mathbf{U}^t , for the MIMO radar using Sub-algorithm 1.
 - 4: Compute the transmit and receive beamformers for the MIMO communication network, \mathbf{F}_j^t and \mathbf{W}_j^t , using Sub-algorithm 2, while using the optimal values for \mathbf{V}^t and \mathbf{U}^t obtained in the previous step as initialization values.
 - 5: Iteratively project the solution of Sub-algorithm 1 on the solution subspace of Sub-algorithm 2 and continue alternatively until convergence at the outer tier level for both ρ and \mathcal{R}_{sum} .
 - 6: Update the iteration index to $t + 1$;
 - 7: **end while**
 - 8: **Output:** The optimum solution $\{\mathbf{U}^*, \mathbf{V}^*, \mathbf{W}_j^*$, and $\mathbf{F}_j^*\}$
-

systems, respectively and the outer-tier represents Algorithm 1. Additionally, Algorithm 1 is based on alternative projection on the convex sets that represent the solution spaces of both Sub-algorithm 1 and Sub-algorithm 2 until a global convergence is obtained. This eventually leads to the optimal transmit and receive beamformers which are needed for the two systems to satisfy peaceful co-existence in their shared spectrum scenario.

D. Convergence and Initialization

This subsection discusses some key points related to the proposed algorithm and sub-algorithms in subsections from III-A to III-C. Specifically, the focus is on the variable initialization, convergence of algorithm/sub-algorithms, execution method, and knowledge of the CSI and the beamforming constraints. We have confirmed through heuristic simulations that obtaining a global optimum solution for the proposed framework is highly likely, even when using initially the identity matrices as beamforming matrices. As the iterative algorithms are exploited to maximize the design objectives, that are, the radar SINR and communication sum-rate, different initializations for the two Sub-algorithms 1, and 2 may lead to different SINR and sum-rate values. The numerical results, which will be provided in Section IV, prove the effectiveness of random initializations. Accordingly, multiple simulation runs of Algorithm 1 which internally contain the two sub-algorithms, should be made with different initializations to obtain the most likely accurate results. The convergence results and analysis are more slightly highlighted in Section IV. Sub-algorithms 1 and 2 are guaranteed to converge because the objective functions are bounded and, at each iteration of these sub-algorithms, they are monotonically moving toward that bound. Generally, AO algorithms are not guaranteed to converge to a global optimum except with the objective functions that own some convexity-like characteristics [31] that our proposed algorithm/sub-algorithms did not prove to own. Finally, the convergence of the cost function does not automatically translate to transmit and receive beamforming convergence. But this issue is beyond the scope of this work and will be addressed in our future research.

E. Avoiding Sum-Rate Saturation Via Distributed Power Control

In sum-rate optimization and IA communication scenarios, the sum-rate performance may saturate at very high SNR levels where IA becomes infeasible [17], [20], [22], [41]. In order to obtain sum-rate performance that scales almost linearly with SNR, the system should somehow restore the IA feasibility. One approach to achieve that is by shutting down a subset of the transmission streams to obtain perfect IA in very high SNR ranges [41], which is known as distributed power control (DPC). The DPC technique introduced in [41] can be implemented in our proposed framework in order to keep the feasibility of IA at high SNR levels. This in turn enables us to prevent sum-rate saturation and maintain full DoFs of the integrated radar and communication system.

IV. SIMULATION RESULTS

In this section, we present numerical results that demonstrate the merits of the proposed TTAO-based spectrum sharing framework. Throughout this part, the proposed framework is compared with the spectrum sharing solution that based on NSP [11]–[14]. Consider a MIMO radar system with a collocated ULA of half wavelength inter-element spacing, and transmitting Gaussian orthogonal waveforms [7]. Assume that the coefficients of the channels, \mathbf{H}_{ij} , are i.i.d. circularly symmetric complex Gaussian, i.e., $\mathcal{CN}(0, \sigma_C^2)$, with $\sigma_C^2 = 1$. Meanwhile, consider that the interference channels \mathbf{G}_{Ri} and \mathbf{G}_{jR} are also circularly symmetric complex Gaussian Rayleigh fading channels with i.i.d. coefficients drawn from $\mathcal{CN}(0, \sigma_R^2)$. Here, we study two cases of interference channels, namely weak interference channels with $\sigma_R^2 = 0.01$, and strong interference channels with $\sigma_R^2 = 1$. Furthermore, consider that there are four stationary targets ($L = 4$), which are located in the far-field with pathloss 2×10^{-3} . The communication system is represented in the form of K – user interference channel, which can easily be adapted to the case of multi-cell communication system. In our simulations, the parameters of communication system are given as $K = 4$ and $d = \min(N, M)$. We assume that the noise power at each communication receiver is normalized to unity. Since, we are assuming that all users have identical transmission power, namely p_C . Then, p_C indicates the communication signal-to-noise ratio (SNR) in the considered scenario. Our simulation results are averaged over 200 channel realizations.

As explained in Section IV, the proposed spectrum sharing framework consists mainly of two parts/sub-algorithms. One part aims at maximizing the SINR at the MIMO radar receiver, while the second part aims at maximizing the total sum-rate in (bits/sec/Hz) at the communication receivers. The main algorithm allows these two sub-algorithms to run sequentially to jointly compute the transmit and receive beamforming matrices for the two systems to optimize their figure of merits. The first part of our simulations concentrates on the convergence issues of all parts of the proposed framework both with weak and strong interference channels.

Fig. 4 shows the convergence curves of the SINR at radar receiver for different numbers of the array elements. It is clear from the figure that Sub-algorithm 1 converges faster in scenarios with smaller number of elements in the arrays. In other words, the convergence rate of the proposed sub-algorithm is inversely proportional to the size of the antenna arrays.

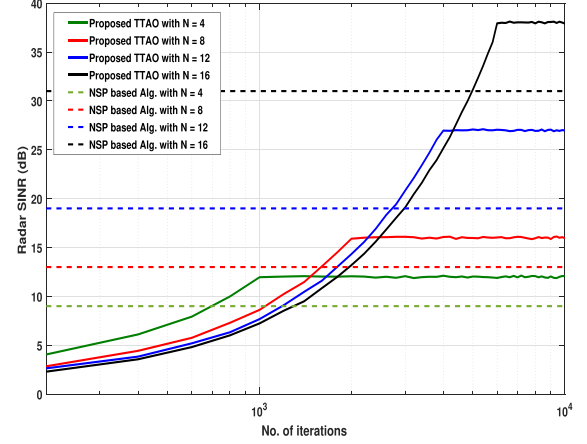


Fig. 4. Convergence curves of the radar receiver SINR achieved by the proposed Sub-algorithm 1 in case of weak interference channels ($\sigma_C^2 = 1$, and $\sigma_R^2 = 0.01$), compared with NSP-based scheme for different array sizes, $M = N = 4, 8, 12, 16$.

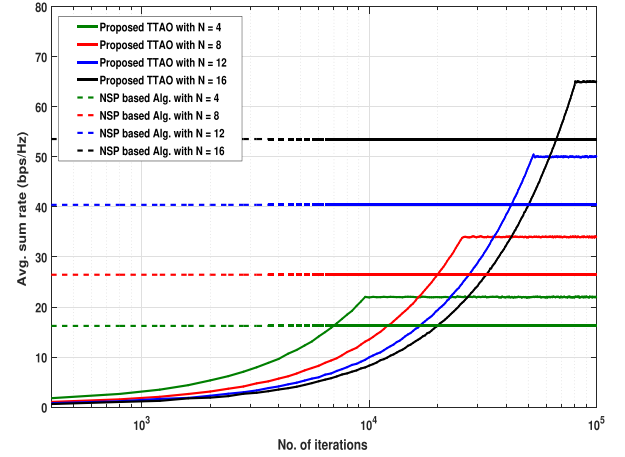


Fig. 5. Convergence curves of the average communication system sum-rate achieved by the proposed Sub-algorithm 2, compared with NSP-based scheme for different array sizes in case of weak interference channels ($\sigma_C^2 = 1$ and $\sigma_R^2 = 0.01$), $M = N = 4, 8, 12, 16$.

Conversely, the converged values itself is directly proportional to the array size. Specifically, the greater the array size, the higher will be the SINR at the radar receiver. A final comment on this figure is that, Sub-algorithm 1 converges at SINR values higher than that achieved with the NSP-based solution. Additionally, the difference in SINR values between Sub-algorithm 1 and the NSP-based scheme becomes greater as the array size becomes larger, for instance 3 dB with array size $N = 4$ and more than 6 dB with array size $N = 16$. The convergence curves for the NSP-based solution are horizontal lines because it is not an iterative approach in nature. The comparison proves the superiority of the proposed sub-algorithm by achieving higher SINR values when converged. Thanks to IA which is able to mitigate all the interference signals generated by different transmitters of the communication system instead of nulling only the strongest interference source as the NSP-based scheme does.

Fig. 5 displays the convergence of the averaged sum-rate with the number of iterations for different sizes of the antennas

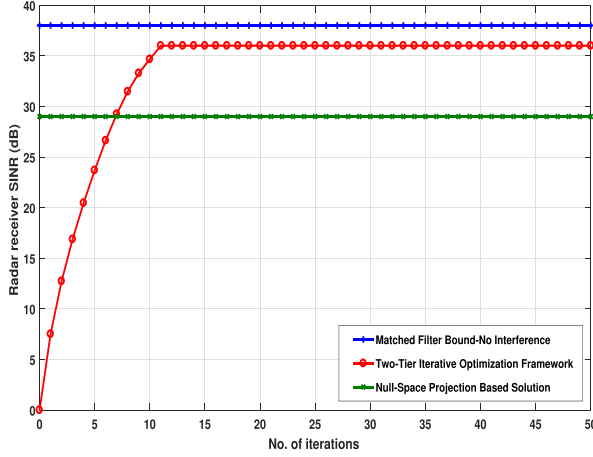


Fig. 6. SINR convergence behavior of the whole TTAO spectrum sharing framework in case of weak interference channels. Number of iterations here, represents the number of iterations the proposed Algorithm 1 takes until convergence. The simulations are done for weak interference channels with $\sigma_C^2 = 1$ and $\sigma_R^2 = 0.01$.

arrays at both the radar transmitter and receiver in case of weak interference channels. Note that the total system sum-rate can be calculated as:

$$\mathcal{R}_{sum} = \sum_{j=1}^K \log_2 \left| \mathbf{I} + \frac{\frac{p_C}{d} \mathbf{W}_j^* \mathbf{H}_{jj} \mathbf{F}_j^* \mathbf{F}_j^* \mathbf{H}_{jj}^* \mathbf{W}_j^*}{\mathbf{W}_j^* \mathbf{B}_j \mathbf{W}_j^*} \right| \quad (30)$$

where the value of \mathbf{B}_j in the denominator of (30) is calculated using (12). As observed in Fig. 5, Sub-algorithm 2 converges to sum-rate values far higher than its NSP counterparts at all array size values, namely $N = 4, 8, 12$, and 16 . Specifically, at $N = 16$ the proposed sub-algorithm achieves a sum-rate value that is 11 bits/sec/Hz higher than the value achieved by the NSP-based scheme. It should be noted that the convergence rate of the proposed Sub-algorithm 1 becomes slower as the array size increases while achieving much better sum-rate. The superior performance of the proposed framework in terms of the sum-rate is due to the ability of the IA scheme to mitigate both the inter-user interference signals arising from the communication side as well as the interference originated due to the existence of the MIMO radar.

Fig. 6 plots the convergence behavior of the TTAO framework, namely Algorithm 1. The results show that the proposed framework achieves much higher SINR values at the radar receiver than that provided by the NSP approach and slightly lower than the optimum matched filter solution in the case of no interference. It must be noted that the horizontal axis, namely the number of iterations, is different from that mentioned in Figs. 4 and 5. The number of iterations in Fig. 6 represents the number of runs of Algorithm 1 until reaching convergence and each iteration includes several iterations of both Sub-algorithm 1 and Sub-algorithm 2. It can be noted that the proposed spectrum sharing framework needs at least 10 iterations to fully converge to the optimal solution.

The results displayed in both Figs. 7 and 8 show the effect of the proposed TTAO spectrum sharing framework on the performance of the MIMO communication network in terms of the total achievable network sum-rate. Additionally, the performance of the proposed framework is tested under different

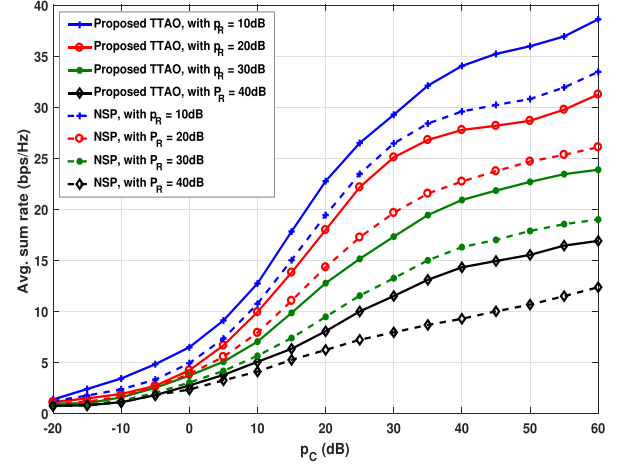


Fig. 7. The total system sum-rate vs SNR of the communication transmitters in case of weak interference channels ($\sigma_C^2 = 1$ and $\sigma_R^2 = 0.01$), the communication transmit power normalized with respect to the noise power, namely p_C . The achievable total system sum-rate is tested at different levels of radar transmit power, $p_R = 10, 20, 30$, and 40 and compared with the NSP-based spectrum sharing solution. $N = M = 8$.

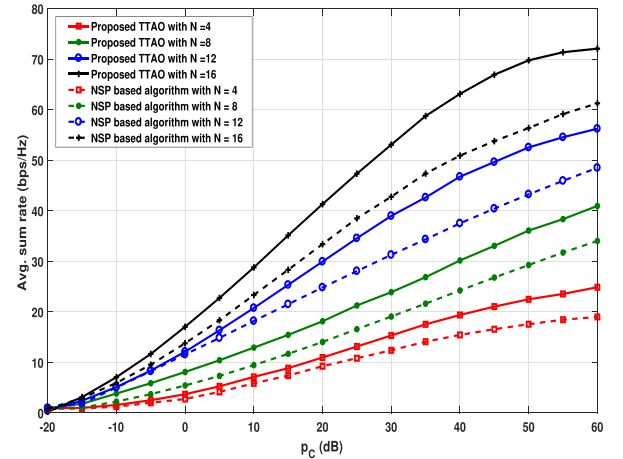


Fig. 8. The total system sum-rate vs SNR of the communication transmitters in case of weak interference channels ($\sigma_C^2 = 1$ and $\sigma_R^2 = 0.01$), the communication transmit power normalized with respect to the noise power, namely p_C . The achievable total system sum-rate is tested at different array sizes, $N = M = 4, 8, 12$, and 16 and compared with the NSP-based spectrum sharing solution.

array sizes of the MIMO radar transmitters as well as the communication transmitters, and is also evaluated for different radar transmitting power levels. In Fig. 7, the results show that even with the existence of radar system in close proximity with different transmit power levels, the proposed framework is still able to mitigate the interference signals. But, it is obvious that, the amount of leakage interference that deliberate to the useful subspaces increases with increasing the radar transmit power level. In spite of that, the proposed framework is still able to achieve higher sum-rate levels compared to the NSP-based spectrum sharing scheme at different levels of the radar transmit power.

Fig. 8 shows the scalability effect of the array size on the sum-rate of MIMO communication network when sharing the spectrum with the MIMO radar. The scalability of the array size leads to the growth of the degrees of freedom (DoFs) achieved

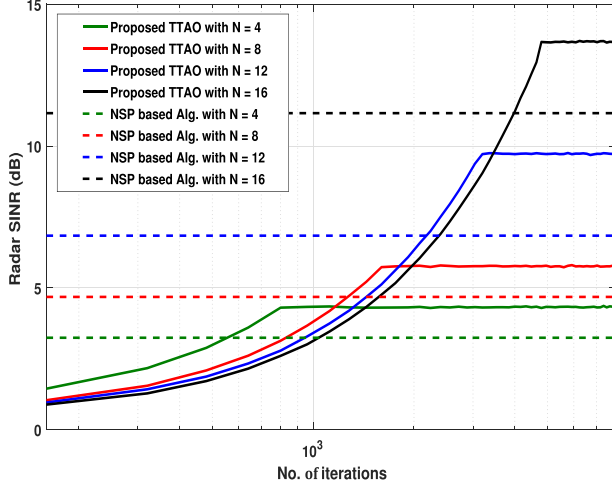


Fig. 9. Convergence curves of the radar receiver SINR achieved by the proposed Sub-algorithm 1 in case of strong interference channels ($\sigma_C^2 = \sigma_R^2 = 1$), compared with NSP-based scheme for different array sizes, $M = N = 4, 8, 12, 16$.

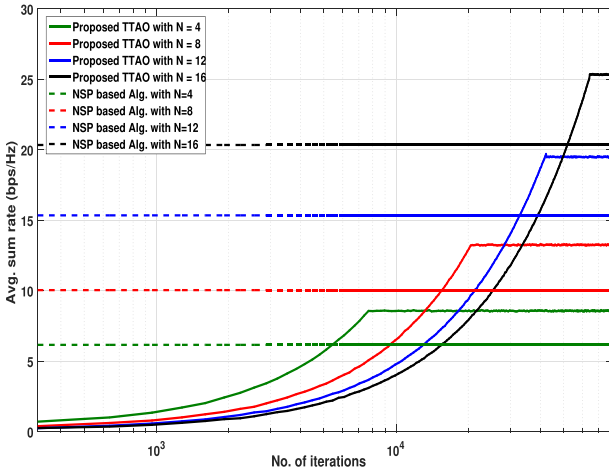


Fig. 10. Convergence curves of the average communication system sum-rate achieved by the proposed Sub-algorithm 2 in case of strong interference channels ($\sigma_C^2 = \sigma_R^2 = 1$), compared with NSP-based scheme for different array sizes, $M = N = 4, 8, 12, 16$.

with the IA and, accordingly, this makes the total sum-rate of the system to increase as a result of increasing the DoFs at the communication receivers. As IA achieves much more interference mitigation effect than the NSP approach, the sum-rate levels achieved using the IA-based TTAO approach is fairly greater than that achieved by the NSP-based approach at any size of antennas array.

In order to test the performance of the proposed spectrum sharing framework in stronger interference channels, the same parameter settings in Figs. 4–8 will be employed, except the channels \mathbf{G}_{iR} and \mathbf{G}_{jR} which are drawn from $\mathcal{CN}(0, 1)$. It is seen in Figs. 9–13 that the proposed framework is still able to provide the best performance for the two systems. It should be noted that due to the stronger interference channel, interference signals might deliberate into the signal subspaces which in turn degrades the performance of the IA approach. However, if

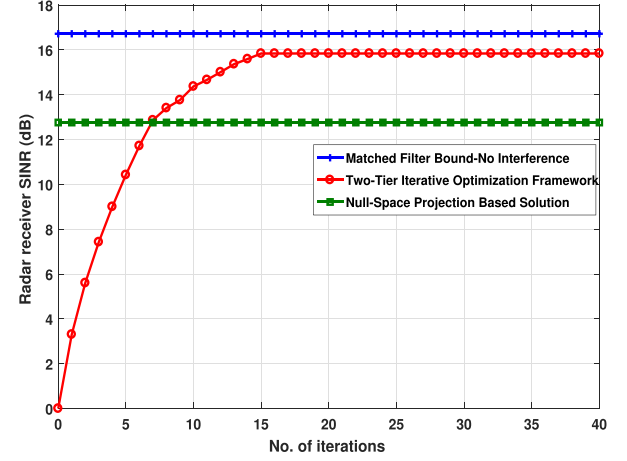


Fig. 11. SINR convergence behavior of the whole TTAO spectrum sharing framework in case of strong interference channels ($\sigma_C^2 = \sigma_R^2 = 1$). Number of iterations here, represent the number of iterations the proposed algorithm 1 take until convergence.

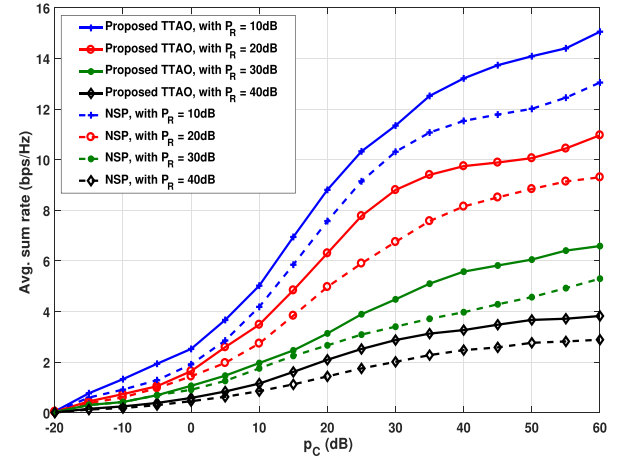


Fig. 12. The total system sum-rate vs SNR of the communication transmitters in case of strong interference channels, the communication transmit power normalized with respect to the noise power, namely p_C . The achievable total system sum-rate is tested at different levels of radar transmit power, $p_R = 10, 20, 30$, and 40 and compared with the NSP-based spectrum sharing solution. $N = M = 8$, and $\sigma_C^2 = \sigma_R^2 = 1$.

the interference channels become further stronger, the receiver is able to decode the interference and cancel it out perfectly [37]–[38]. As seen in Figs. 7, 8, 12, and 13, the optimal DoF values are not achieved indicating that the system is in infeasible region for IA. As an indication of the superiority of the proposed framework in both feasible and infeasible regions of the IA conditions, the results in Fig. 14 are obtained under the same parameters settings as those in Fig. 12 except that the DPC technique [40], [41] is adopted in our proposed framework to guarantee the applicability of IA and utilization of full-DoFs at high SNR levels. It is clear from Fig. 14 that the sum-rate saturation effect shown in Fig. 12 is completely removed. Moreover, the proposed TTAO approach is superior to the conventional NSP scheme in terms of averaged sum-rate, clearly indicated in Fig. 14. This is because the proposed strategy is able to utilize the full DoFs of the system.

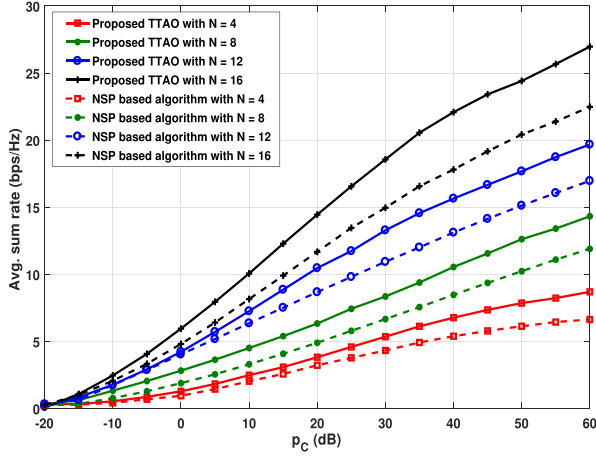


Fig. 13. The total system sum-rate vs SNR of the communication transmitters in case of strong interference channels, the communication transmit power normalized with respect to the noise power, namely p_C . The achievable total system sum-rate is tested at different array sizes, $N = M = 4, 8, 12$, and 16 and compared with the NSP-based spectrum sharing solution. $\sigma_C^2 = \sigma_R^2 = 1$.

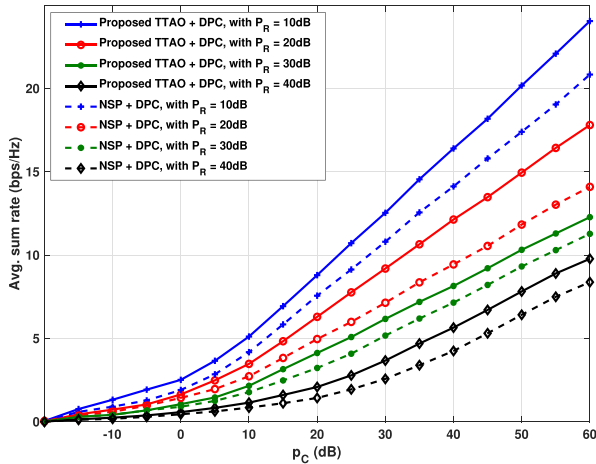


Fig. 14. Averaged sum-rate versus p_C with DPC to keep achieving full DoFs and help restoring the feasibility of IA at high SNR levels. The total system sum-rate vs SNR of the communication transmitters in case of strong interference channels. The used simulation parameters and conditions are the same as that used in Fig. 13.

Finally, to highlight the improved performance gained due to the coordination between the two systems through the centralized architecture, the proposed framework will be compared with the state-of-the-art approaches in the case of no coordination between the systems, namely, selfish communication/radar scenarios. This scenario refers to the situation where the two systems operate in close proximity but they are oblivious to one another. In this scenario, the communication system maximizes the total sum-rate based on IA criteria without any concern about the interference it causes to the radar system. Additionally, the MIMO-radar system maximizes its SINR based on uniform precoding $\mathbf{V} = \sqrt{dP_R}/M\mathbf{I}$, NSP precoding, and transmit-receive beamforming obtained by solving (13) with the first terms in both (14) and (17) equal to zero, without any concern to the interference exerted by the communication system. It is obvious from Fig. 15 that the SINR at the radar receiver achieved

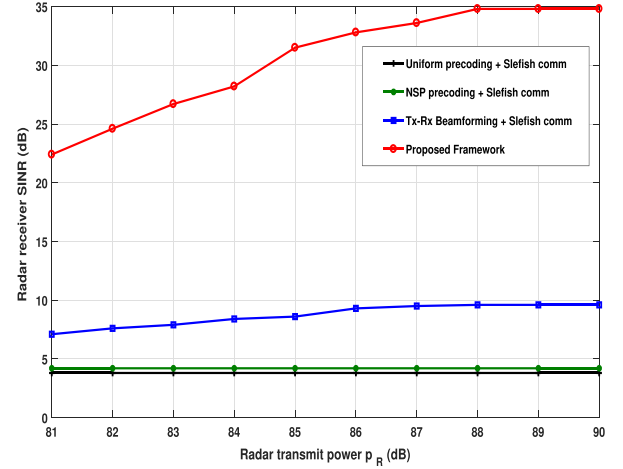


Fig. 15. The radar SINR vs radar transmit power P_R . Comparison between the proposed spectrum sharing framework with full coordination between MIMO radar and MIMO communication systems and the state-of-the-art approaches with selfish communication. $M = 8$, and $N = 4$.

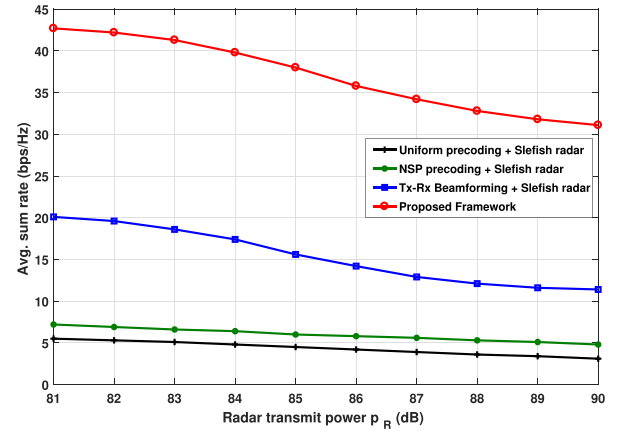


Fig. 16. The average sum rate vs radar transmit power P_R . Comparison between the proposed spectrum sharing framework with full coordination between MIMO radar and MIMO communication systems and the state-of-the-art approaches with selfish communication. $M = 8$ and $N = 4$.

with the proposed framework, that is based on full coordination between the two systems, is much higher than any other approaches, under selfish communication condition. On the other hand, the average sum rate at communication side is also affected severely due to the interference from a selfish radar. As shown in Fig. 16, the average sum rate of the communication system obviously decreases by not less than 20 bps/Hz due to the lack of coordination between the two systems.

V. CONCLUSION

We have presented a spectrum sharing framework for peaceful co-existence between a collocated MIMO radar and a MIMO communication network. The key solution to achieve an optimal performance for the two systems, is the use of an intelligent interference mitigation strategy. The tailored IA approach in this work, which is achieved through employing transmit and receive beamformers at both the MIMO radar and the MIMO communication systems, has been proved to be a promising technique for

this mission. We have formulated the spectrum sharing framework into an iterative AO algorithm that alternates between two other iterative sub-algorithms to jointly compute the optimum transmit and receive beamforming filters that achieve the optimum figure of merit values for both MIMO radar and MIMO communication systems. Our simulation results guarantee the convergence of the proposed framework. The proposed framework is shown to provide a superior performance to the NSP-based schemes for both radar and communication systems, in terms of higher SINR and average system sum-rate, respectively. As a future work, we would address the impact of CSI errors on both the MIMO radar and MIMO communication provided that they are sharing the same spectrum band. Specifically, we would model the CSI errors and develop robust version of the proposed framework.

APPENDIX A

PROOF OF THE SUM RATE GRADIENT

Let us denote $\mathbf{F}_j = \sqrt{\beta_j} \tilde{\mathbf{F}}_j$, where β_j is defined by:

$$\beta_j = \frac{P_C}{\text{Tr}(\tilde{\mathbf{F}}_j^\dagger \tilde{\mathbf{F}}_j)} \text{ for } j = 1, \dots, K$$

So, the sum rate function can be written as:

$$\mathcal{R}_{sum} = \sum_{i=1}^K \log_2 \left| \mathbf{I} + \beta_j \mathbf{H}_{ij} \tilde{\mathbf{F}}_j \tilde{\mathbf{F}}_j^\dagger \mathbf{H}_{ij}^\dagger \left(\sum_{i \neq j}^K \beta_j \left(\frac{P_R}{P_C} \right) \times \mathbf{H}_{ij} \tilde{\mathbf{F}}_j \tilde{\mathbf{F}}_j^\dagger \mathbf{H}_{ij}^\dagger + P_R \mathbf{G}_{iR} \mathbf{V}_i \mathbf{V}_i^\dagger \mathbf{G}_{iR}^\dagger + \sigma_C^2 \mathbf{I} \right)^{-1} \right|$$

Based on Eqs. (25) and (26), the above sum rate equation can be expressed as:

$$\mathcal{R}_{sum} = \sum_{i=1}^K \log_2 |\Phi_i| - \log_2 |\Pi_i|$$

Since the sum rate \mathcal{R}_{sum} is a real valued function, the gradient of the sum rate with respect to $\tilde{\mathbf{F}}_j$, namely, $\nabla_{\tilde{\mathbf{F}}_j} \mathcal{R}_{sum} = 2\partial \mathcal{R}_{sum} / \partial \tilde{\mathbf{F}}_j^*$. Then, using the fact that $d(\ln |\mathbf{X}|) = \text{Tr}\{\mathbf{X}^{-1} d(\mathbf{X})\}$, the differential of the sum rate with respect to $\tilde{\mathbf{F}}_j^*$ is given as:

$$d\mathcal{R}_{sum} = \frac{1}{\ln 2} \sum_{i=1}^K \text{Tr} \left(\Phi^{-1} \left(d\beta_j \mathbf{H}_{ij} \tilde{\mathbf{F}}_j \tilde{\mathbf{F}}_j^\dagger \mathbf{H}_{ij}^\dagger + \beta_j \mathbf{H}_{ij} d\tilde{\mathbf{F}}_j \tilde{\mathbf{F}}_j^\dagger \mathbf{H}_{ij}^\dagger \right) \right) - \frac{1}{\ln 2} \sum_{j \neq i}^K \text{Tr} \left(\Pi^{-1} \left(d\beta_j \mathbf{H}_{ij} \tilde{\mathbf{F}}_j \tilde{\mathbf{F}}_j^\dagger \mathbf{H}_{ij}^\dagger + \beta_j \mathbf{H}_{ij} d\tilde{\mathbf{F}}_j \tilde{\mathbf{F}}_j^\dagger \mathbf{H}_{ij}^\dagger \right) \right)$$

Also, using $d\{\text{Tr}(\mathbf{X})\} = \text{Tr}\{d(\mathbf{X})\}$, $\text{Vec}(d\mathbf{X}) = d\text{Vec}(\mathbf{X})$, $\text{Tr}(\mathbf{X}^T \mathbf{Y}) = \text{Vec}(\mathbf{X})^T \text{Vec}(\mathbf{Y})$, and $\text{Tr}(\mathbf{X} d\mathbf{Y}^\dagger) = \text{Tr}(\mathbf{X}^T$

$d\mathbf{Y}^*)$ [39], the above equation can be rewritten as:

$$d\mathcal{R}_{sum} = \left[\frac{\beta_j}{\ln 2} \sum_{i=1}^K \text{Vec} \left(\mathbf{H}_{ij}^\dagger \Phi_i^{-1} \mathbf{H}_{ij} \tilde{\mathbf{F}}_j \right)^T - \frac{\beta_j^2}{P_C \ln 2} \sum_{i=1}^K \text{Tr} \left(\tilde{\mathbf{F}}_j^\dagger \mathbf{H}_{ij}^\dagger \Phi_i^{-1} \mathbf{H}_{ij} \tilde{\mathbf{F}}_j \right) \text{Vec} \left(\tilde{\mathbf{F}}_j \right)^T - \frac{\beta_j}{\ln 2} \sum_{j \neq i}^K \text{Vec} \left(\mathbf{H}_{ij}^\dagger \Pi_i^{-1} \mathbf{H}_{ij} \tilde{\mathbf{F}}_j \right)^T + \frac{\beta_j^2}{P_C \ln 2} \sum_{j \neq i}^K \text{Tr} \left(\tilde{\mathbf{F}}_j^\dagger \mathbf{H}_{ij}^\dagger \Pi_i^{-1} \mathbf{H}_{ij} \tilde{\mathbf{F}}_j \right) \text{Vec} \left(\tilde{\mathbf{F}}_j \right)^T \right] d\text{Vec} \left(\tilde{\mathbf{F}}_j^* \right).$$

where, we have used $d\beta_j = -\beta_j^2 \text{Tr}(\tilde{\mathbf{F}}_j d\tilde{\mathbf{F}}_j^\dagger) / P_C$. Note that, the coefficients of $d\text{Vec}(\tilde{\mathbf{F}}_j^*)$ in the above equation leads to the derivative $\partial \mathcal{R}_{sum} / \partial \tilde{\mathbf{F}}_j^*$. After normalizing the precoding vector through multiplying by $\ln 2 / 2$, the gradient of the sum rate $\nabla_{\mathbf{F}_j} \mathcal{R}_{sum}$ is then derived as in (24).

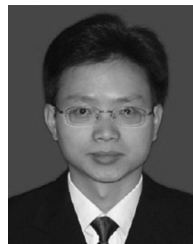
REFERENCES

- [1] A. Osseiran *et al.*, "The foundation of the mobile and wireless communications system for 2020 and beyond: Challenges, enablers and technology solutions," in *Proc. IEEE 77th Veh. Technol. Conf.*, 2013, pp. 1–5.
- [2] G. Ku and J. M. Walsh, "Resource allocation and link adaptation in LTE and LTE-advanced: A tutorial," *IEEE Comm. Surveys Tuts.*, vol. 17, no. 3, pp. 1605–1633, Third Quarter 2015.
- [3] L. Lu, G. Y. Li, A. L. Swindlehurst, A. Ashikhmin, and R. Zhang, "An overview of massive MIMO: Benefits and challenges," *IEEE J. Sel. Topics Signal Process.*, vol. 8, no. 5, pp. 742–758, Oct. 2014.
- [4] L. Dai, B. Wang, Y. Yuan, S. Han, C. I. I, and Z. Wang, "Non-orthogonal multiple access for 5G: Solutions, challenges, opportunities, and future research trends," *IEEE Comm. Mag.*, vol. 53, no. 9, pp. 74–81, Sep. 2015.
- [5] Federal Communications Commission (FCC), "FCC proposes innovative small cell use in 3.5 GHz band," Dec. 2012.
- [6] G. Locke and L. E. Strickling, "An assessment of the near-term viability of accommodating wireless broadband systems in the 1675–1710 MHz, 1755–1780 MHz, 3500–3650 MHz, and 4200–4220 MHz, 4380–4400 MHz bands," Tech. Rep. TR-13-490, US Dept. Commerce. Nat. Telecommun. Inf. Admin., Washington, DC, USA, 2012.
- [7] B. Li, A. P. Petropulu, and W. Trappe, "Optimum co-design for spectrum sharing between matrix completion based MIMO radars and a MIMO communication system," *IEEE Trans. Signal Process.*, vol. 64, no. 17, pp. 4562–4575, Sep. 2016.
- [8] B. Li and A. P. Petropulu, "Joint transmit designs for coexistence of MIMO wireless communications and sparse sensing radars in clutter," *IEEE Trans. Aerosp. Electron. Syst.*, vol. 53, no. 6, pp. 2846–2864, Dec. 2017.
- [9] C. Kopp, "Search and acquisition radars (S-band, X-band) Tech. Rep. APA-TR-2009-0101," Apr. 2012. [Online]. Available: <http://www.ausairpower.net/APA-Acquisition-GCL.html>. Accessed on: Mar. 2018.
- [10] A. Goldsmith, *Wireless Communications*. Cambridge, U.K.: Cambridge Univ. Press, 2005.
- [11] S. Sodagari, A. Khawar, T. C. Clancy, and R. McGwier, "A projection based approach for radar and telecommunication systems co-existence," in *Proc. IEEE Global Commun. Conf.*, 2012, pp. 5010–5014.
- [12] A. Khawar, A. Abdelhadi, and T. C. Clancy, "Spectrum sharing between S-band radar and LTE cellular system: A spatial approach," in *Proc. IEEE Int. Symp. Dyn. Spectr. Access Netw.: SSPARC Workshop*, Apr. 2014, pp. 7–14.
- [13] D. Tse and P. Viswanath, *Fundamentals of Wireless Communication*. Cambridge, U.K.: Cambridge Univ. Press, 2005.
- [14] A. Babaei, W. H. Tranter, and T. Bose, "A null space-based precoder with subspace expansion for radar/communications co-existence," in *Proc. Signal Process. Commun. Symp. - Glob. Commun. Conf.*, 2013, pp. 3487–3492.

- [15] K. Singh, S. Biswas, T. Ratnarajah, and F. Khan, "Transceiver design and power allocation for full-duplex MIMO communication systems with spectrum sharing radar," *IEEE Trans. Cogn. Commun. Netw.*, vol. 4, no. 3, pp. 556–566, Sep. 2018.
- [16] F. Liu, C. Masouros, A. Li, T. Ratnarajah, and J. Zhou, "MIMO radar and cellular coexistence: A power-efficient approach enabled by interference exploitation," *IEEE Trans. Signal Process.*, vol. 66, no. 14, pp. 3681–3695, May 2018.
- [17] C. M. Yetis, G. Tiengao, S. A. Jafar, and A. H. Kayran, "On feasibility of interference alignment in MIMO interference networks," *IEEE Trans. Signal Process.*, vol. 58, no. 9, pp. 4771–4782, Sep. 2010.
- [18] C. Y. Chen and P. P. Vaidyanathan, "MIMO radar waveform optimization with prior information of the extended target and clutter," *IEEE Trans. Signal Process.*, vol. 57, no. 9, pp. 3533–3544, Sep. 2009.
- [19] Jun Liu, Hongbin Li, and Brahim Himed, "Joint optimization of transmit and receive beamforming in active arrays," *IEEE Signal Process. Lett.*, vol. 21, no. 1, pp. 39–42, Jan. 2014.
- [20] K. Gomadam, V. R. Cadambe, and S. A. Jafar, "A distributed numerical approach to interference alignment and applications to wireless interference networks," *IEEE Trans. Inf. Theory*, vol. 57, no. 6, pp. 3309–3322, Jun. 2011.
- [21] H. Sung, S. H. Park, K. J. Lee, and I. Lee, "Linear precoder designs for K-user interference channels," *IEEE Trans. Wireless Commun.*, vol. 9, no. 1, pp. 291–301, Jan. 2010.
- [22] V. R. Cadambe and S. A. Jafar, "Interference alignment and degrees of freedom of the K-user interference channel," *IEEE Trans. Inf. Theory*, vol. 54, no. 8, pp. 3425–3441, Aug. 2008.
- [23] N. Zhao, F. Richard Yu, M. Jin, Q. Yan, and V. C. M. Leung, "Interference alignment and its applications: A survey, research issues, and challenges," *IEEE Commun. Surveys Tuts.*, vol. 18, no. 3, pp. 1779–1803, Third Quarter 2016.
- [24] C. Suh, M. Ho, and D. N. Tse, "Downlink interference alignment," *IEEE Trans. Commun.*, vol. 59, no. 9, pp. 2616–2626, Sep. 2011.
- [25] K. Lee, "Uplink interference alignment for two-cell MIMO interference channels," *IEEE Trans. Veh. Technol.*, vol. 62, no. 4, pp. 1861–1865, May 2013.
- [26] W. Shin, W. Noh, K. Jang, and H. Choi, "Hierarchical interference alignment for downlink heterogeneous networks," *IEEE Trans. Wireless Commun.*, vol. 11, no. 12, pp. 4549–4559, Dec. 2012.
- [27] M. Rihan, M. Elsabrouty, O. Muta, and H. Furukawa, "Interference mitigation framework based on interference alignment for femtocell-macrocell two tier cellular systems," *IEICE Trans. Comm.*, vol. E98-B, no. 3, pp. 467–476, Mar. 2015.
- [28] B. Guler and A. Yener, "Selective interference alignment for MIMO cognitive femtocell networks," *IEEE J. Sel. Areas Commun.*, vol. 32, no. 3, pp. 439–450, Mar. 2014.
- [29] X. Rao, L. Ruan, and V. K. Lau, "Limited feedback design for interference alignment on MIMO interference networks with heterogeneous path loss and spatial correlations," *IEEE Trans. Signal Process.*, vol. 61, no. 10, pp. 2598–2607, May 2013.
- [30] A. Beck, "On the convergence of alternating minimization for convex programming with applications to iteratively reweighted least squares and decomposition schemes," *SIAM J. Optim.*, vol. 25, no. 1, pp. 185–209, Jan. 2015.
- [31] I. Csiszar and G. Tusnady, "Information geometry and alternating minimization procedures," *Stat. Decis.*, vol. 1, pp. 205–237, 1984.
- [32] J. A. Mahal, A. Khawar, A. Abdelhadi, and T. C. Clancy, "Spectral coexistence of MIMO Radar and MIMO Cellular System," *IEEE Trans. Aerosp. Electron. Syst.*, vol. 53, no. 2, pp. 655–668, Apr. 2017.
- [33] C. Zhang, X. Li, H. Yin, and G. Wei, "Interference alignment precoder design on Grassmann manifold for cellular system," in *Proc. IEEE Int. Conf. Commun. China*, 2012, pp. 568–572.
- [34] A. Edelman, T. A. Arias, and S. T. Smith, "The geometry of algorithms with orthogonality constraints," *SIAM J. Matrix Anal. Appl.*, vol. 20, no. 2, pp. 303–353, 1998.
- [35] A. Khawar, A. Abdelhadi, and C. Clancy, "Target detection performance of spectrum sharing MIMO radars," *IEEE Sensors J.*, vol. 15, no. 9, pp. 4982–4940, Sep. 2015.
- [36] J. Li and P. Stoica, *MIMO Radar Signal Processing*. New York, NY, USA: Wiley, 2008.
- [37] H. Sato, "The capacity of the gaussian channel under strong interference," *IEEE Trans. Inf. Theory*, vol. 27, no. 6, pp. 786–788, Nov. 1981.
- [38] M. H. M. Costa and A. A. El Gamal, "The capacity region of the discrete memoryless interference channel with strong interference," *IEEE Trans. Inf. Theory*, vol. 33, no. 5, pp. 710–711, Sep. 1987.
- [39] J. R. Magnus and H. Neudecker, *Matrix Differential Calculus With Applications in Statistics and Econometrics*. New York, NY, USA: Wiley, 2002.
- [40] Z. K. M. Ho and D. Gesbert, "Balancing egoism and altruism on interference channel: The MIMO case," in *Proc. Int. Commun. Conf.*, 2010, pp. 1–5.
- [41] Z. K. M. Ho, M. Kaynia, and D. Gesbert, "Distributed power control and beamforming on MIMO interference channels," in *Proc. Eur. Wireless Conf.*, 2010, pp. 654–660.



Mohamed Rihan received the B.Sc. (hons.) degree in electronics and communication engineering from Menoufia University, Al Minufya, Egypt. He received the M.Sc. and Ph.D. degrees in electronics and communication engineering from Egypt-Japan University of Science and Technology, New Borg El Arab, Egypt, in 2012 and 2015 respectively. From 2014 to 2015, he was a Researcher with the Department of Advanced Information Technology, Graduate School of ISEE, Kyushu University, Fukuoka, Japan. From 2016 to 2017, he was an Adjunct Professor at the Center of Photonics and Smart Materials, Zewail City of Science and Technology, Giza, Egypt. He is currently a Postdoctoral Research Fellow with the College of Information Engineering, Shenzhen University, Shenzhen, China. He is also serving as an Assistant Professor with the Faculty of Electronic Engineering, Menoufia University. His research interests include massive MIMO and mmWave communications, interference alignment, resource allocation, cognitive heterogeneous networks, and applications of signal processing in wireless communications.



Lei Huang (M'07–SM'14) was born in Guangdong, China. He received the B.Sc., M.Sc., and Ph.D. degrees in electronic engineering from Xidian University, Xi'an, China, in 2000, 2003, and 2005, respectively. From 2005 to 2006, he was a Research Associate with the Department of Electrical and Computer Engineering, Duke University, Durham, NC, USA. From 2009 to 2010, he was a Research Fellow with the Department of Electronic Engineering, City University of Hong Kong, and a Research Associate with the Department of Electronic Engineering, Chinese University of Hong Kong. From 2011 to 2014, he was a Professor with the Department of Electronic and Information Engineering, Harbin Institute of Technology Shenzhen Graduate School. Since 2014, he has been with the College of Information Engineering, Shenzhen University, where he is currently a Distinguished Professor. His research interests include spectral estimation, array signal processing, statistical signal processing, and their applications in radar, and navigation and wireless communications. He has been on the editorial boards of the IEEE TRANSACTIONS ON SIGNAL PROCESSING (2015-present), Elsevier-Digital Signal Processing (2012-present), and IET Signal Processing (2017-present). He has been an elected member of the Sensor Array and Multichannel Technical Committee of the IEEE Signal Processing Society (2016-present). He was elected an IET Fellow in 2018.